Interaction with the membrane uncovers essential differences between highly homologous GPCRs

Sayan Mondal*, George Khelashvili*, Jennifer M. Johnston, Davide Provasi**, Hao Wang**, Olaf S. Andersen*, Marta Filizola**, Harel Weinstein***

*Department of Physiology and Biophysics, Weill Cornell Medical College, Cornell University, New York, NY

**Department of Structural and Chemical Biology, Mount Sinai School of Medicine, New York, NY

I. Abstract

The lipid membrane environment has been shown to play a significant role in the function and organization of G-protein coupled receptors (GPCRs) and other transmembrane proteins. We now show quantitatively how small sequence differences between otherwise highly homologous GPCRs can result in strikingly different membrane interaction characteristics. This is evidenced by comparing the membrane interactions of two pairs of functionally related family A GPCRs - (1) the beta1 and beta2 adrenergic receptors; and, (2) the kappa- and delta- opioid receptors, embedded in a lipid bilayer composed of a 16:0-18:1 PC (POPC) /10% Cholesterol mixture. We used the recently described 3D Continuum-Molecular Dynamics (3D-CTMD) approach (Ref. 1) to quantify the membrane deformation profile and corresponding energy costs due to the hydrophobic mismatch. The novel computational method accounts for the irregular hydrophobic surface of the protein and the hydrophobic mismatch at particular TMs that is not alleviated by membrane deformations. A description of the irregular membrane-protein interface from MD simulations of protomeric receptors with the coarse-grained Martini force field provided the information on the membrane-protein boundary needed to quantify with 3D-CTMD the energetics of membrane deformation for each system. The specific residues involved in unfavorable polar-to-hydrophobic interactions not alleviated by membrane deformations at each TM were identified from solvent accessibilities in the MD trajectories. We found strikingly different energy costs of hydrophobic mismatch at TMs 4,5 between the beta1 and beta2 adrenergic receptors. In contrast, both kappa and delta opioid receptors exhibited a similar pattern of (small) energy cost around the protein with slightly more pronounced residual mismatch at TM4. These distinct patterns of energy differences indicate how small sequence differences in otherwise homologous GPCRs can affect the mechanisms driving their organization in the cell membrane.

II. Aim and Rationale

The general goal is to gain molecular-level insight into the participation of the membrane in GPCR function and organization.

(1) GPCRs are found to spontaneously oligomerize on reconstitution into liposomes without need for cellular machinery but with specific organization (refs. 2,3).

(2) Rhodopsin oligomerizes to different extents in lipid bilayers of different hydrophobic thickness (refs. 4,5).

(3) Even homologous GPCRs such as ß1-adrenergic receptor (ß1AR) and ß2 -adrenergic receptor (ß2AR) differ in the extent and/ or stability of the oligomerization in the membrane (ref. 6).

III. Working Hypothesis

The difference between highly homologous GPCRs involves differential interaction with the membrane.

IV. Background: GPCR-membrane interactions

In response to a mismatch with the hydrophobic length of the protein, the lipid bilayer deforms locally around the protein to alleviate the mismatch.

Fig. 1 Membrane deformation profile for rhodopsin in the thinner di(C14:1)PC lipid bilayer and the thicker di(C20:1)PC lipid bilayer (taken from ref. 1).

However, a complete hydrophobic matching may not be attained due to the adjacent positioning of polar and hydrophobic residues at certain TMs. The **residual exposure is a major component of the energy penalty** due to hydrophobic mismatch.

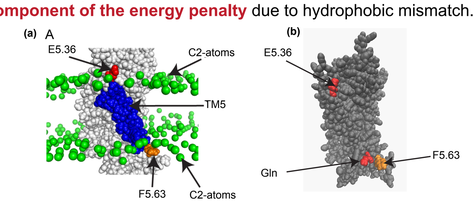

Residual Energy Penalty ~ 5.4 kT at TM5

Fig. 2 (a) Illustration of **residual exposure** at transmembrane segment (TM) 5 of rhodopsin in di(C14:1)PC lipid bilayer (taken from ref. 1). The hydrophobic F5.63 is exposed to unfavorable hydrophobic-polar interaction. Note: a polar residue at position 5.63 would have no residual exposure in the thin di(C14:1)PC bilayer. **(b)** The hydrophobic matching at F5.63 is limited by the adjacent location of a Gln.

V. Method

To quantify the energy penalty due to hydrophobic mismatch for two pairs of homologous GPCRs (1) ß1AR and ß2AR, (2) δ-opioid receptor (DOR) vs. κ-opioid receptor (KOR), we applied a combined continuum-molecular dynamics approach that takes into account the irregular hydrophobic surface of the protein and the residual exposure (detailed description in Mondal (2011) et al. Biophys J 101 (9): 2092-2101, see reprint). The molecular dynamics simulations were performed with the Martini force field. The starting structures of the ß-adrenergic receptors were obtained from respective crystal structures (refs. 7-9) and the DOR and KOR from homology models (see ref. 10 for details).

VI. Results

ß1AR vs. ß2AR: Sequence comparison identifies positions that could mediate different interaction with the membrane

Despite the high sequence similarity in the TM-bundle, ß1AR and ß2AR have residues with different hydrophobic character near the ends of TM4 and TM5.

ß1-adrenergic receptor (ß1AR) vs ß2-adrenergic receptor(ß2AR)

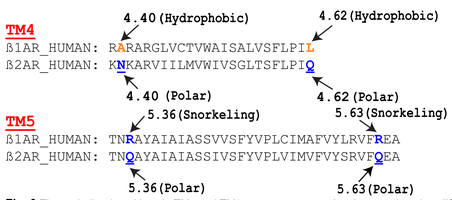

Fig. 3 The underlined positions in TM4 and TM5 represent putative key molecular differences between ß1AR and ß2AR in terms of membrane-protein interaction

Therefore, there is an intriguing possibility that the the homologous ß1AR and ß2AR may differ in their residual exposure profile.

Residual exposure occurs at TMs 4,5 in ß2AR, but not in ß1AR

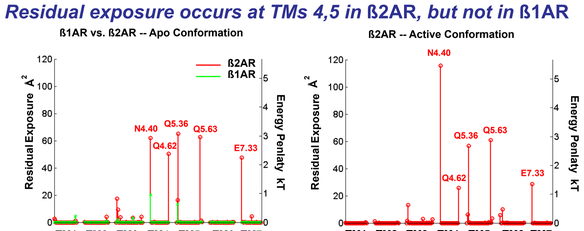

Fig. 4 Residual exposure profile for ß1AR vs. ß2AR in POPC/ 10% Chol bilayer. It quantifies the surface area of the residues involved in unfavorable hydrophobic-polar interactions. The corresponding energy penalties taken to be linearly proportional to the surface area. **Note the distinct residual exposure between ß1AR vs. ß2AR at the putative sites identified in figure 3 (and in TM7).** The large residual exposure at TMs 4,5 of ß2AR occurs in its inactive as well as its active conformations (corresponding to respective crystal structures).

The residual exposure profiles identify key residue-level differences between ß1AR vs. ß2AR

The residual exposure profile is explained by considering the key residues in their structural context

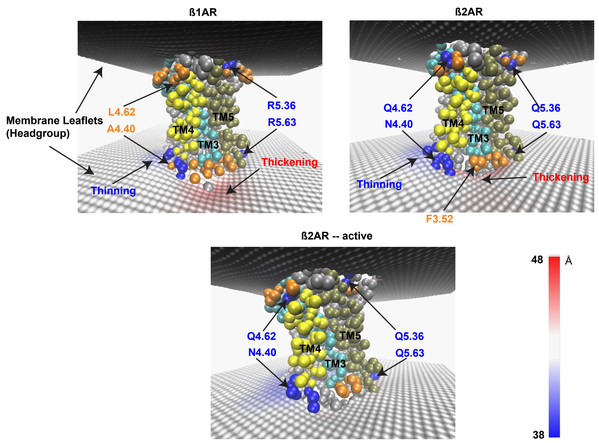

Fig. 5 The time-averaged, spatially smoothed headgroup profile of the upper and lower leaflets from each MD trajectory along with a snapshot of the corresponding protein. The colormap represents the bilayer thickness. Red regions of the bilayer indicate thickening and blue regions thinning of the membrane. Polar residues are colored in blue and hydrophobic residues are in orange. TM3 is highlighted in cyan, TM4 in yellow, and TM5 in tan.The energy cost due to the membrane deformation is evaluated to be < 2kT in all cases.

Neighboring hydrophobic residues (orange above, e.g., F3.52) and polar residues (blue) drive the bilayer in opposite direction, to both thicken and thin, in the same neighborhood. This limits the extent of hydrophobic matching, leaving some residual exposure.

Negative control: When hydrophobicity at TMs 4,5 is similar in the two GPCRs

DOR vs. KOR: Sequence comparison shows that the residues at the key positions in TMs 4,5 have similar hydrophobic character

Fig. 6 Sequence comparison between DOR and KOR shows **similar (hydrophobic) residues at the key positions 4.40, 4.62, and 5.63.** At the remaining key position 5.36, DOR has a polar Threonine, but it does not interact with the membrane, as illustrated in the next figure.

Structural context of these residues also suggests similar residual exposure at TMs 4,5 of DOR and KOR in POPC/ 10% Chol bilayer

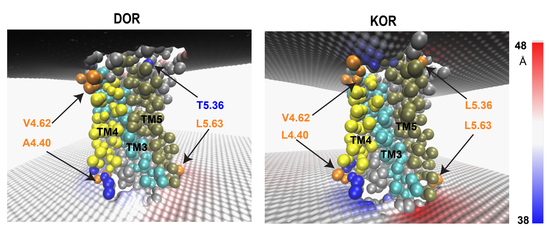

Fig. 7 Illustration of the residues at the key positions in their structural context and in relation to the membrane environment. The colormap shows the deformed membrane thickness around the protein. The hydrophobic residues are in orange and polar residues in blue. Note that TM4 of both DOR and KOR have a hydrophobic residue (4.40) sandwiched between two polar residues.

DOR vs. KOR: Similar residual exposure at TMs 4,5

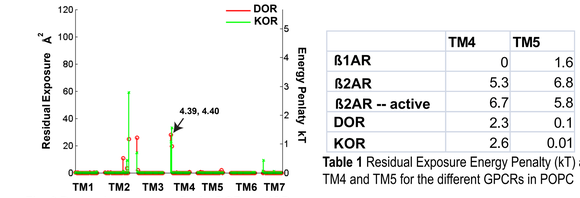

	TM4	TM5
ß1AR	0	1.6
ß2AR	5.3	6.8
ß2AR -- active	6.7	5.8
DOR	2.3	0.1
KOR	2.6	0.01

Table 1 Residual Exposure Energy Penalty (kT) at TM4 and TM5 for the different GPCRs in POPC

Fig. 8 Residual exposure profile for DOR vs. KOR.

Thus, unlike *ß1AR* and *ß2AR*, DOR and KOR have similar interaction with the membrane at TMs 4,5

Participation of Membrane in GPCR oligomerization

From molecular dynamics simulations of diffusion-reaction with the Martini force field, we find that ***ß2AR GPCRs spontaneously oligomerize in the POPC bilayer*** (as expected).

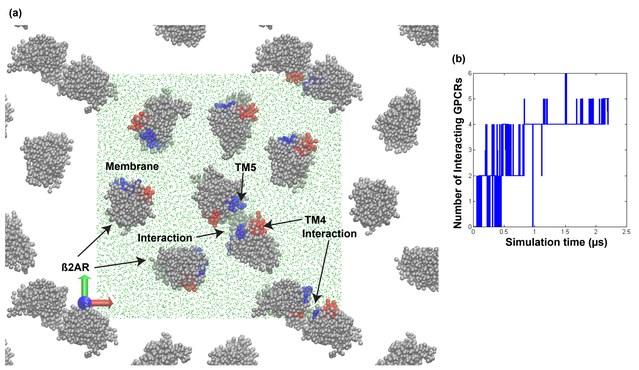

Fig. 9 (a) An illustrative snapshot from the trajectory of nine ß2AR GPCRs in POPC at a lipid/ protein ratio of ~ 110:1 (currently > 2 µs long). The periodic image of the simulation cell is also shown for completeness. The membrane (green) is shown in thre simulation cell only. The orientation of each protein is indicated by highlighting TM4 (red) and TM5 (blue) in the simulation cell. (b) The number of interacting GPCRs (< 5 Å distance) over the course of the trajectory.

Oligomerization interactions involve residues that are critical for membrane-protein interaction

In fig. 5, F3.52 was identified in connection to the residual exposure profile of ß2AR, as part of the hydrophobic cluster near the key polar residues with residual exposure in TM4 and TM5

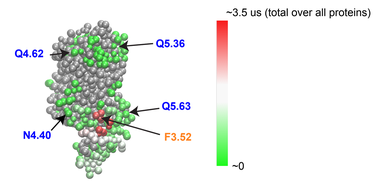

Fig. 10 (a) Heatmap highlighting the residues of ß2AR involved in oligomerization interaction (criteria: < 5 Å from the interacting protomer). In red are the residues mediating interaction with other receptors over long periods of time (total over all proteins during the course of the trajectory).

The spontaneous oligomerization interactions involve a number of residues and possibly complex local interactions. However, to understand the participation of the membrane in the oligomerization, we focus on the key residues based on the molecular-level analysis of the interaction of the monomer with the membrane.

Residual exposure is alleviated at several residues in the spontaneously formed oligomeric constructs

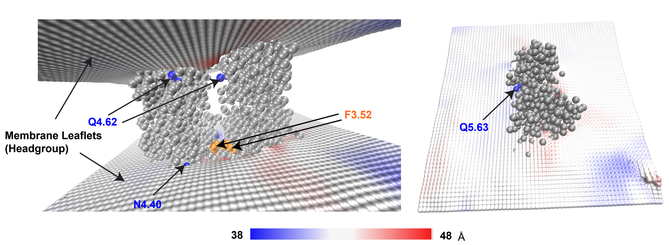

Fig. 10 (b) A snapshot of a dimeric B2AR construct involving F3.52 that emerges from the simulation, embedded in the time-averaged and spatially smoothed membrane surrounding this dimeric construct. Note that the dimerization interface alleviates the residual exposure at Q4.62. Furthermore, the membrane is able to alleviate the residual exposure in the neighboring region of F3.52 (e.g., at N4.40 and Q5.63).

The simulation suggests that the residual exposure may be alleviated in two ways during oligomerization:

(1) by directly occluding the offending residue within the interface (e.g., Q4.62 above), and

(2) by reducing the energetic drive for the membrane to both thicken and thin in the same neighborhood in order to alleviate hydrophobic mismatch with nearby polar and hydrophobic residues (e.g., F5.32 participates in the oligomerization interface, and interacts less with the membrane).

VII. Conclusions

- Sequence-level differences in interaction with the membrane indentify key positions in homologous GPCRs responsible for membrane-driven effects.
- Such effects include GPCR oligomerization, by which the energy penalty due to hydrophobic mismatch is alleviated.

VIII. References

1. Mondal S, Khelashvili G, Shan J, Andersen OS, Weinstein H (2011). Biophysical J 101:2092-2101
2. Mansoor S, Palczewski K, Farrens DL (2006). PNAS 103: 3060-3065
3. Fung JJ,...,Kobilka BK (2009). EMBO 28:3315-3328
4. Botelho AV, .. , Brown MF (2006). Biophysical J 4464-4477
5. Periole X, .. , Sakmar TP (2007). JACS 129: 10126-10132
6. Dorsch S,..., Bunemann M (2009). Nature Methods 6: 225 -230
7. Warne T, ...,Schertler GF (2008). Nature 454:486-491
8. Cherezov V, ..., Stevens RC (2007). Nature 450:383-387
9. Rasmussen SG, ..., Kobilka BK (2011). Nature 469:175-180
10. Johnston JM,...,Filizola M (2011). Biochemistry 50:1682-1690

Acknowledgements

This work was supported by the NIH grants DA012408, DA012923, and U54 GM087519, and the computational resources of the Institute for Computational Biomedicine at Weill Cornell Medical College of Cornell University.